

Response of dust on thermal emission spectra observed by Planetary Fourier Spectrometer (PFS) on-board Mars Express (MEX)

J. Masoom^{a,b}, S A Haider^{a*} & Marco Giuranna^c

^aPlanetary Sciences Division, Physical Research Laboratory, Navrangpura, Ahmedabad 380009, India

^bResearch Scholar, Faculty of Science, Pacific Academy of Higher Education and Research University, Udaipur 313003, India

^cIstituto di Astrofisica e Planetologia (IAPS), Istituto Nazionale di Astrofisica (INAF)
Viale del Fosso del Cavaliere, Roma 1000133, Italy

Received 8 May 2018; accepted 8 February 2019

The thermal emission spectra have provided many useful insights about the Martian atmosphere and surface. The interpretation of the thermal emission spectra can give us information about atmospheric temperature, pressure, mineralogy and presence of atmospheric constituents including their isotopes. In the present work, we have analysed the thermal emission data for dust storm season on Mars. The signature of dust in the thermal emission spectra for Martian Year (MY) 28 confirm the presence ($L_s=280^\circ$ and 300°) and the absence ($L_s=240^\circ$ and 320°) of the dust storm at latitude range 0° - 10° S, 10° - 20° S and 20° - 30° S. We have compared our results with earlier mission data with thermal emission measurements made by Planetary Fourier Spectrometer (PFS) on-board Mars Express (MEX) between wave numbers 250 - 1400 cm^{-1} . We have observed features at wave numbers 600 - 750 cm^{-1} and 900 - 1200 cm^{-1} due to absorptions by CO_2 and dust respectively. We have obtained brightness temperatures from thermal emission spectra by inverting the Planck function. The maximum brightness temperature $\sim 280^\circ\text{ K}$ was measured at $L_s=240^\circ$ when Mars received a large amount of solar radiation at perihelion. The minimum brightness temperature $\sim 220^\circ\text{ K}$ was observed at $L_s=320^\circ$ in the absence of dust storm. In presence of dust storm, thermal emission spectra and brightness temperatures were reduced by factors of ~ 3.0 and ~ 1.3 , respectively, between wave numbers 900 - 1200 cm^{-1} in comparison to that observed in absence of dust storm.

Keywords: Mars atmosphere, Dust Storm

1 Introduction

The infrared spectroscopy is an important remote sensing technique to study the planetary atmospheres and surfaces. Over several decades this technique has been used on Mars to study the composition of the surface, minerals, dust, water ice clouds, temperature and atmospheric gases¹⁻³. The atmosphere of Mars consists of several CO_2 bands, weak water vapour lines, radiatively active water ice clouds, and signatures of dust periodically stirred up by strong surface winds. The surface of Mars can be observed in certain spectral windows: 780 - 1000 cm^{-1} , 1080 - 1240 cm^{-1} and 2500 - 2800 cm^{-1} . The Mariner 9, Viking, Mars Global Surveyor (MGS), Mars Odyssey and Mars Express (MEX) have observed the presence of water and dust on the surface of Mars from infrared thermal emission spectrometer¹⁻³. These missions have also observed surface minerals, rocks and temperatures on Mars.

The dust storms can develop in few hours and spread over the entire planet within few days⁴. It

affects the densities, temperatures, and winds of the Mars' atmosphere. It has been found that large dust storms on Mars grow in the tropics of southern hemisphere during spring/summer⁵. The modeling studies have suggested that the Martian dust storms are capable of generating a significant amount of electricity which split CO_2 and H_2O into CO , OH , O and H . These elements recombine into H_2O_2 and can fall on the ground as a snow that would destroy organic molecules associated with life⁶. The dust is an effective absorber of solar radiation, which provides a major source of heating, thus generating vertical and horizontal winds. There have been reported many dust storms⁴⁻⁶. We have studied the response of a dust storm on the thermal emission spectra and brightness temperature that were observed⁷ by Planetary Fourier Spectrometer (PFS) onboard MEX in MY28. These measurements were carried out at low latitude region (0 - 30° S) for $L_s=240^\circ$, 280° , 300° and 320° corresponding to orbits # 4338, 4552, 4670 and 4808 respectively. It is found that the thermal emission spectra and brightness temperature are

*Corresponding author (Email: haider@prl.res.in)

decreased by a factor of ~ 3 due to absorption of dust between wave numbers $900\text{-}1200\text{ cm}^{-1}$.

2 Planetary Fourier Spectrometer

Recently MEX carried out PFS instrument for the measurement of thermal emission spectra emitted by the surface/atmosphere of Mars. This instrument has a short-wavelength (SW) channel covering the spectral range $1700\text{-}8200\text{ cm}^{-1}$ ($1.2\text{-}5.5\text{ }\mu\text{m}$) and long wavelength (LW) channel covering $250\text{-}1700\text{ cm}^{-1}$ ($5.5\text{-}45\mu\text{m}$)⁸⁻¹⁰. In SW channel of PFS spectra, methane was first discovered by Formisano *et al.*¹¹ at wave number 3018 cm^{-1} . They have reported global average of methane mixing ratio to be 10 ± 5 ppbv. Later Geminale *et al.*^{12,13} studied the seasonal, diurnal and spatial variations of methane in the atmosphere of Mars. Recently Sindoni *et al.*¹⁴ have observed mixing ratios of water vapour and carbon monoxide at wave numbers 3845 cm^{-1} ($2.6\text{ }\mu\text{m}$) and 4235 cm^{-1} ($2.36\text{ }\mu\text{m}$) respectively. They have found anti-correlation between the concentrations of water vapour and CO. This is due to sublimation of the carbon dioxide and water vapour from north polar ice cap, which decreases concentration of non-condensable species CO. Similar process also occurs in south polar cap but in this case the condensation of carbon dioxide and water vapour increases the concentration of non-condensable species CO.

Zasova *et al.*¹⁵ reported preliminary results of temperature profiles, dust and water ice cloud opacities retrieved from thermal infrared spectrum of PFS. They have identified orographic ice clouds above Olympus and Ascraeus Mons. Giuranna *et al.*¹⁶ studied the mechanisms of CO₂ condensation and accumulation over south polar cap of Mars. They found that the polar cap expands symmetrically with a constant speed during the fall season. Mättänen *et al.*¹⁷ analysed PFS data to study the response of local dust storm on atmospheric thermal structure near the equator of Mars in the late northern summer. They reported that the temperatures were about $\sim 10\text{ K}$ colder near the surface and $\sim 5\text{ K}$ warmer in the upper atmosphere during the dust storm period. Sato *et al.*¹⁸ investigated tidal variations in the atmospheric temperature at low altitude ($<45\text{ km}$) during the dust-clear period from PFS data. Montabone *et al.*¹⁹ analysed the data obtained from MGS and Odyssey for MY24 to MY32 and studied the inter-annual and seasonal variability of dust optical depths. Aoki *et al.*²⁰ have reported H₂O₂ in the Martian

atmosphere at wave number 379 cm^{-1} . They have derived mixing ratios 16 ± 19 ppb at $L_s = 0^\circ\text{-}120^\circ$, 35 ± 32 ppb at $L_s = 120^\circ\text{-}240^\circ$ and 41 ± 28 ppb at $L_s = 240^\circ\text{-}360^\circ$. It is found that the emission intensity and temperature decrease by factors of ~ 3 and 1.3 , respectively, during dust storm period.

3 Datasets and Analysis

In this paper we have analysed PFS data of LW channel for MY28 when a major dust storm occurred at low latitude in southern hemisphere between $L_s = 260^\circ\text{-}300^\circ$ for about a couple of weeks. The thermal emission spectra and brightness temperature were retrieved from these observations in absence and presence of dust storm. The observed thermal emission spectra were characterized by Planck function at the corresponding surface temperature under Local Thermodynamic Equilibrium condition (LTE)²¹. The Planck function was expressed as given below:

$$B_T = \frac{2hc^2\nu^3}{\left(e^{\frac{h\nu}{kT}} - 1 \right)} \quad \dots (1)$$

where B_T is the observed thermal emission spectra at brightness temperature T , ν is the wave number, h is Planck constant, k is Boltzmann constant, and c is speed of light. The Planck function is varying with altitudes because the temperature T is altitude dependent. The altitude-dependent of brightness temperature²¹ were calculated by inverting equation (1) as follows:

$$T_B = \frac{h\nu}{k \ln \left(\frac{2hc^2\nu^3}{B_T + 1} \right)} \quad \dots (2)$$

The propagation of radiation in the planetary atmospheres is influenced by absorption, emission and scattering by molecular species. In the above Eqs (1) and (2) we have not considered molecular scattering under LTE condition. Planck function cannot produce spectral features of the emission spectra of PFS. The spectral features of the thermal emission spectra can be reproduced by radiative transfer equation including scattering by atmospheric molecules. Our aim is not to

reproduce the spectral features of thermal emission spectra by radiative transfer model. Therefore, we have obtained brightness temperature directly from the observed thermal emission spectra²¹ by inverting Planck function.

The PFS also observed instrumental error while measuring thermal emission spectra. This error depends upon the measurement conditions and mechanical and non-mechanical vibration of the spacecraft. *Comolli and Saggin*²² showed that these uncertainties can be reduced by averaging the measured spectra. Giuranna et al.⁷ reported about less than 1% error in PFS observations. We have averaged PFS data over 10 degree latitudes between 0° to 30°S to decrease the instrumental noise²².

4 Results and Discussion

In Fig. 1 (a & b), we have shown measured optical depth of dusts as a function of latitude and Ls for MY 28 (Fig.1a represents a contour plot of dust opacity of MY28 at different Ls between latitudes -90°S and +90°N. Figure.1b shows variations of dust opacity with Ls for MY28 at latitude range 0°-10°S, 10°-20°S and 20°-30°S). These observations were carried out from nadir direction at infrared wavelength 9.3 μ m from Thermal Emission Imaging System (THEMIS) on board Mars Odyssey²³. The local time of THEMIS observations are limited from 2:00 PM to 6:00 PM because Mars Odyssey is orbiting in a sun-synchronous orbit where Mars would be monitored for a short local time. These optical depths are averaged over

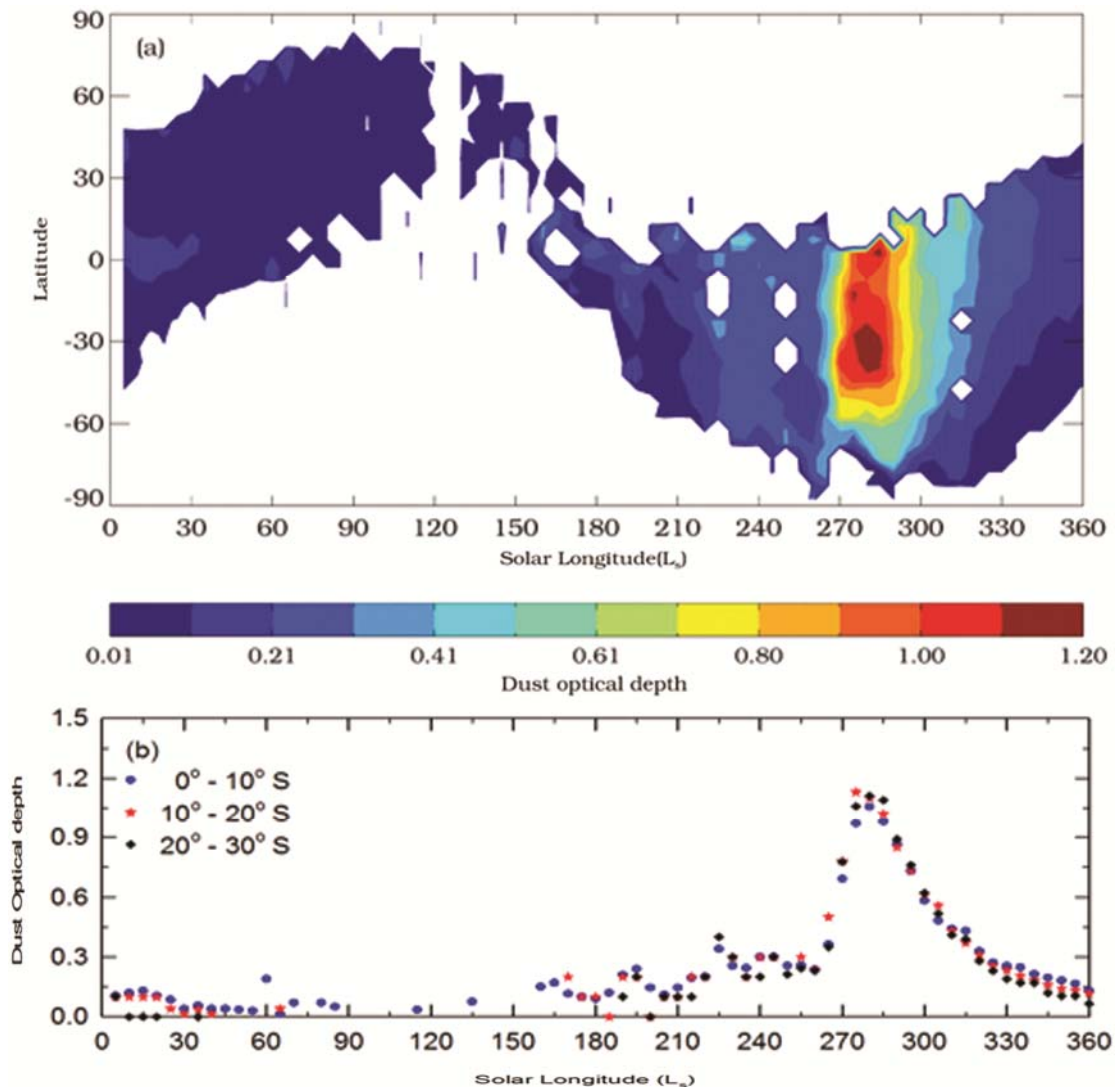


Fig. 1 — (a) Contour plot of dust optical depths (under the colour bar) for MY28 as observed by THEMIS experiment onboard Mars Odyssey at different Ls between -90° S and +90°N and (b) Line plot of dust optical depth variations with Ls for MY28 at latitude range 0°-10°S, 10°-20°S and 20°-30°S.

longitudes. The L_s and latitude values refer to the centre of the $5^\circ \times 5^\circ$ bins. The uncertainties in the optical depths were calculated to be ± 0.03 . A major dust storm was observed in MY28 at low latitude in southern hemisphere of Mars. This dust storm occurred during southern summer ($L_s = 260^\circ$ - 300°) at perihelion when Mars received about 40% more sunlight than the aphelion. In the summer, surface temperature increases which produce high wind velocity to raise the dust above the surface of Mars²⁴. When dust is raised into the atmosphere it forms a thick layer which reduces $9.3 \mu\text{m}$ temperatures that are cooler than the surface temperature. During the dust storm period the value of τ increased to about 1.2 at $L_s=280^\circ$. The τ is the optical depth of the atmosphere during peak dust storm period. There was a little spatial variation in the opacity as the storm decayed ($L_s=300^\circ$). During the decay period of dust storm the optical depths did not change significantly with latitude. Before and after a couple of weeks at $L_s = 240^\circ$ and 320° , the intensity of this dust storm was reduced and τ decreased significantly to 0.1, which we consider background aerosol loading in a clean atmosphere when dust storm is absent.

The Fig. 2 shows the track coverage of PFS measurements in MY28 along four MEX orbits at $L_s = 240^\circ$, 280° , 300° and 320° . We have selected these orbits where MEX passed through southern low latitude region (0 - 30°S) at fixed longitude of Mars. During these orbits the effects of global dust storm were highest. The Fig. 3 (a-c) represents thermal emission spectra measured by PFS instrument between wave numbers 250 - 1400 cm^{-1} at latitude range 0° - 10°S , 10° - 20°S and 20° - 30°S respectively. These spectrum were observed in MY28 at $L_s=240^\circ$, 280° , 300° and 320° corresponding to orbit # 4338, 4552, 4670 and 4808 respectively (The emission spectra is not observed at $L_s=320^\circ$ between latitude

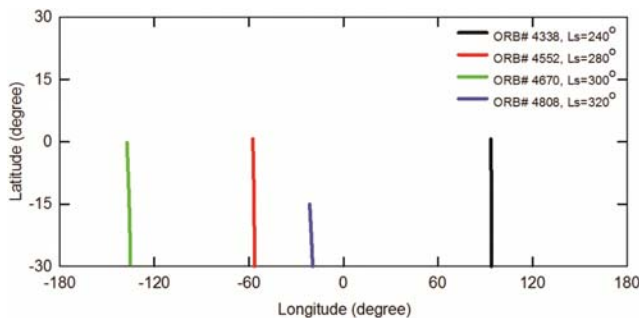


Fig. 2 — Geographical distribution of PFS measurements carried out from MEX for $L_s=240^\circ$, 280° , 300° and 320° during orbit # 4338, 4552, 4670 and 4808 respectively.

range 0 - 10°S). In Table 1 we have summarized the number of PFS spectra used for averaging over latitude range 0° - 10°S , 10° - 20°S and 20° - 30°S at $L_s= 240^\circ$, 280° , 300° and 320° corresponding to orbit # 4338, 4552, 4670 and 4808 respectively.

In these spectra, prominent dip at about 667 cm^{-1} was observed due to absorption of CO_2 . The broad peak at about 300 - 400 cm^{-1} is observed due to absorption of H_2O . The emission intensity decreased by factor of ~ 3 due to absorption of dust between wave number 900 - 1200 cm^{-1} in presence of dust storm. The absorption of dust was maximum during the peak dust storm period at latitude range 10° - 20°S . Several Q-branches¹⁶ have been observed in the emission spectra at wave numbers 545, 596, 618, 667, 720, 742 and 792 cm^{-1} due to CO_2 isotopic molecules $\text{O}^{16}\text{C}^{12}\text{O}^{16}$. The wave numbers in these spectra are chosen at interval 1.5 cm^{-1} . It was found that thermal infrared emission intensities are decreasing with increasing L_s at 240° , 280° and 320° during spring, summer onset and late summer respectively. There was no significant change in the thermal intensities at $L_s=280^\circ$ and 300° because the season was almost same. In summer, the polar caps experienced sublimation due to increase in temperature. The H_2O and CO_2 are condensable gases. The abundances of these gases were large during summer due to sublimation process in comparison to that in spring. The thick atmosphere produced less infrared thermal radiations from the surface of Mars. The thermal emission spectra are not changing significantly with latitudes 0° - 10°S , 10° - 20°S and 20° - 30°S . It produced a flat dip at around 900 - 1200 cm^{-1} due to absorption of dust during storm period at $L_s=280^\circ$ and $L_s=300^\circ$. The effect of dust storm in the emission spectra was not seen in the late spring at $L_s=320^\circ$.

Figure 4 (a-c) represents the brightness temperature profiles between wave numbers 250 - 1400 cm^{-1} at latitude range 0° - 10°S , 10° - 20°S and 20° - 30°S respectively. The brightness temperatures were obtained from the thermal emission spectra shown in Fig. 3 (a-c) by inverting Planck function. In the invert calculation, the non-linearity of Planck function will be eliminated. Therefore, the brightness temperature was nearly same at wave number $\leq 600 \text{ cm}^{-1}$. There was a decrease in brightness temperature due to absorption of dust between wave numbers 900 - 1200 cm^{-1} . When the dust was raised into the atmosphere the day-time temperature decreased because atmospheric layers are cooler than the surface of Mars¹⁶. The major dip in the brightness temperature

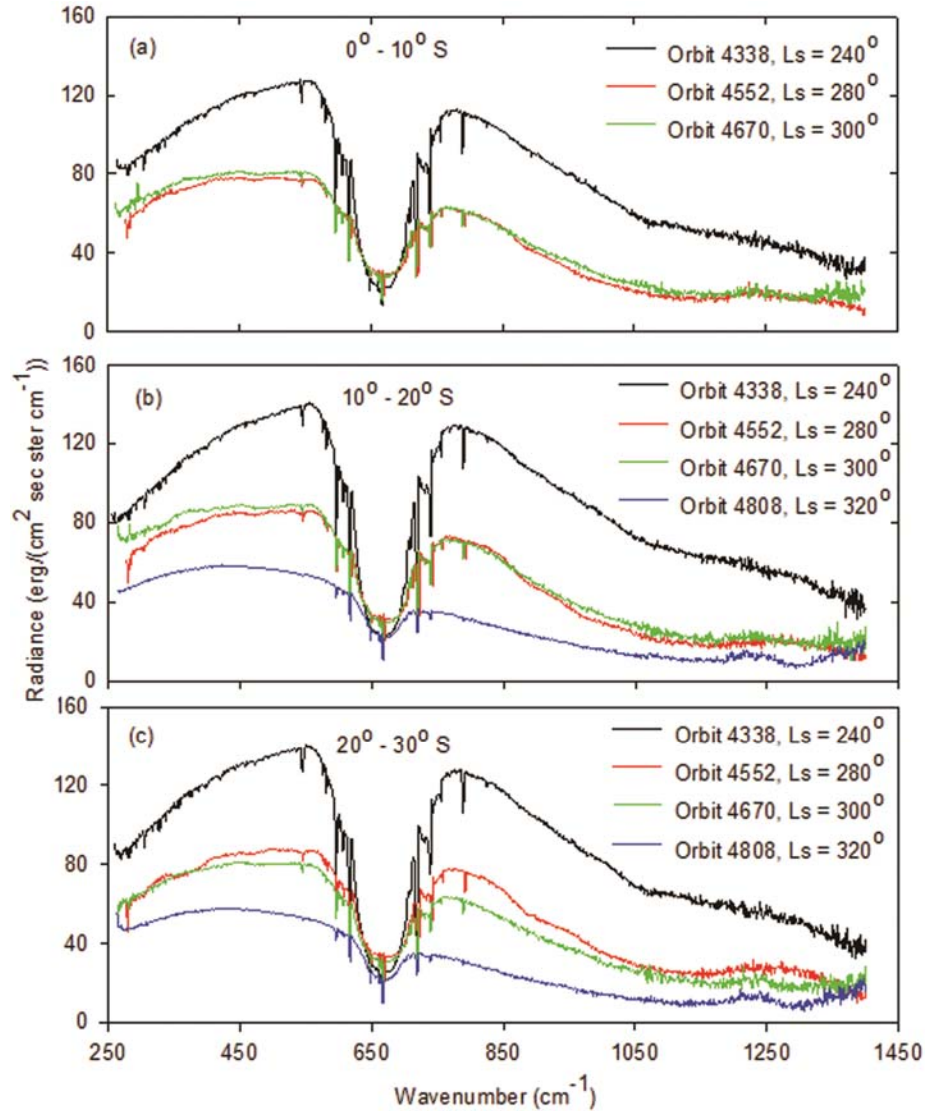


Fig. 3 — The thermal emission spectra observed by PFS instrument during orbit # 4338, 4552, 4670 and 4808 at $L_s=240^\circ$, 280° , 300° and 320° respectively. These emission spectra are averaged over 10° latitude: (a) 0° - 10° S, (b) 10° - 20° S and (c) 20° - 30° S.

Table 1 — Number of spectra used in the averaging of PFS data

Solar longitude Ls	Number of spectra for averaging (Latitude range)		
	0- 10° S	10- 20° S	20- 30° S
240	23	19	19
280	17	25	20
300	24	23	26
320	-	18	15

due to absorption by CO_2 was observed at wave number 667 cm^{-1} . The Q branches of CO_2 isotopic molecules were also seen in the temperature spectra as observed in the infrared thermal emission spectra. The temperature was decreasing with the increasing Ls between wave numbers 250 - 1400 cm^{-1} . The maximum

temperature ~ 260 - 280 K was observed at $L_s=240^\circ$ when Mars reached at perihelion and it received a large amount of solar radiation. The dust storm was observed between summer onset and mid-summer at $L_s=280^\circ$ and 300° , respectively, when Mars was moving away from perihelion. The temperature decreased to $\sim 220 \text{ K}$ during the late summer at $L_s=320^\circ$. In this season a small dip was noticed in the temperature at wave number 1300 cm^{-1} , which was produced due to low emissivity in presence of larger particles of mineral dust near Christiansen frequency²⁴. The PFS instrument observed instrumental noise in the brightness temperature and thermal emission spectra. The noise in the PFS spectrum was produced due to mechanical and non-mechanical vibration of the spacecraft²². Other

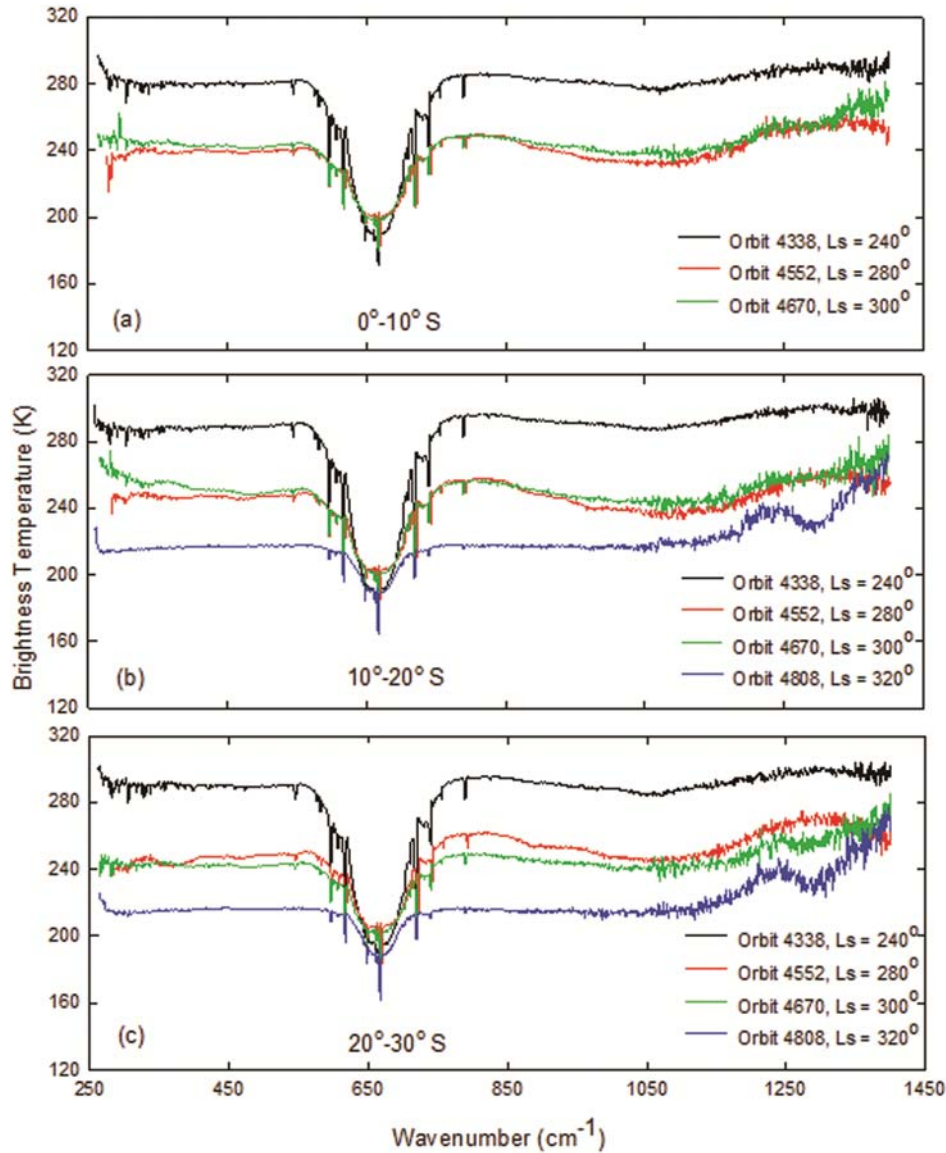


Fig. 4 — The brightness temperature inverted from radiances observed by PFS instrument during orbit # 4338, 4552, 4670 and 4808 at $L_s=240^\circ$, 280° , 300° and 320° respectively. These temperature spectra were averaged over 10° latitude: (a) 0° - 10° S, (b) 10° - 20° S and (c) 20° - 30° S.

sources of errors depend upon the measurement conditions. These errors are less than 1% in the measurements²⁰. The uncertainties produced by various disturbances can be reduced by the averaging of the spectra²². We have averaged PFS spectra at 10° latitude to reduce the random noise. A noise equivalent radiance of 0.2 - 0.4 $\text{erg}/\text{cm}^2/\text{s}/\text{sr}/\text{cm}^{-1}$ was deduced from the repeatability of the calibration spectra taken periodically from deep space and from a built-in blackbody²².

5 Summary and Conclusions

We report an analysis of PFS spectra at low latitude of Mars in presence and absence of dust

storm. The brightness temperature was obtained from thermal emission spectra by inverting the Planck function. The present work reports the effects of dust absorption into the Martian atmosphere and how much it can affect the thermal emissions qualitatively. Four major dust storms⁴ were observed on Mars during MY10, MY13, MY25 and MY28 from Mariner 9, Viking, MGS and MEX respectively. The brightness temperatures were measured during these dust storm periods. In comparing brightness temperatures of MEX observations with the earlier measurements made by Mariner 9, Viking and MGS, we have found substantial increment of about

15°-20°K in the latest measurement. The infrared spectrometers onboard Mariner 9, Viking and MGS have observed maximum brightness temperatures ~ 250° K, ~ 255° K and ~ 265° K in presence of dust storms corresponding to MY10, MY13 and MY25 respectively²⁵⁻²⁷. The PFS onboard MEX has observed maximum and minimum brightness temperatures ~ 280°K and ~ 220°K at Ls = 240° and Ls = 320° respectively in MY28 during the dust storm period. We have found that thermal emission spectrum and temperature were reduced by factors of ~ 3 and ~ 1.3, respectively, during the dust storm period due to absorption of dust between wave numbers 900-1200 cm⁻¹.

Acknowledgement

The authors acknowledge the Principal Investigator Marco Giuranna of the Planetary Fourier Spectrometer (PFS) onboard the Mars Express mission for providing datasets in the archive. Datasets of the Planetary Fourier Spectrometer (PFS) have been downloaded from the ESA Planetary Science Archive (<http://archives.esac.esa.int/psa>). S. A. Haider and J. Masoom acknowledge the support of J. C. Bose grant for supporting to carry out this work.

References

- 1 Hanel R A, Conrath B J, Hovis W A, Kunde V G, Lowman P D, Pearl J C, Prabhakara C, Schlachman B & Levin G V, *Science*, 175 (1972) 305
- 2 Kieffer H H, Martin T Z, Peterfreund A R, Jakosky B M, Miner E D & Palluconi F D, *J Geophys Res*, 82 (1977) 4249.
- 3 Christensen P R, Bandfield J L, Hamilton V E, Ruff S W, Kieffer H H, Titus T N, Malin M C, Morris R V, Lane M D, Clark R L & Jakosky B M, Mars Global Surveyor, *J Geophys Res*, 106 (2001) 23823
- 4 Sheel V & Haider S A, *J Geophys Res*, 121 (2016) 8038.
- 5 Wolkenberg P, Giuranna, M, Grassi D, Aronica A, Aoki S, Scaccabarozzi D & Saggin B, *Icarus*, 310 (2018) 32.
- 6 Kass D M, Kleinbohl, A, McCleese, D J, Schofield, J T, & Smith, M D, *Geophys Res Lett (USA)*, 43 (2016) 6111.
- 7 Giuranna M, Formisano V, Biondi D, Ekonomov A, Fonti S, Grassi D, Hirsch H, Khatuntsev I, Ignatiev N, Malgoska M, Mattana A, Maturilli A, Mencarelli E, Nespoli F, Orfei R, Orleanski P, Piccioni G, Rataj M & Zasova L, *Planet Space Sci*, 53 (2005) 993.
- 8 Formisano V. et al, *Planet Space Sci*, 53 (2005) 963.
- 9 Fouchet T, Lellouch E, Ignatiev N, Forget F, Titov D V, Tschimmel M, Montmessin F, Formisano V, Giuranna M, Maturilli A & Encrenaz T, *Icarus*, 190 (2007) 32.
- 10 Wolkenberg P, Smith M D, *Icarus*, 215 (2011) 628.
- 11 Formisano V, Atreya S, Encrenaz T, Ignatiev N & Giuranna M, *Science*, 306 (2004) 1758.
- 12 Geminale A, Formisano V & Giuranna M, *Planet Space Sci*, 56 (2008) 1194
- 13 Geminale A, Formisano V & Sindoni G, *Planet Space Sci*, 59 (2011) 137.
- 14 Sindoni G, Formisano V & Geminale A, *Planet Space Sci*, 59 (2011) 149
- 15 Zasova L, Formisano V, Moroz V, Grassi D, Ignatiev N, Giuranna M, Hansen G, Blecka M, Ekonomov A, Lellouch E & Fonti S, *Planet Space Sci*, 53 (2005) 1065.
- 16 Giuranna M, Grassi D, Formisano V, Montabone L, Forget F & Zasova L, *Icarus*, 197 (2008) 386.
- 17 Määttänen A, Fouchet T, Forni O, Forget F, Savijärvi H, Gondet B, Melchiorri R, Langevin Y, Formisano V, Giuranna M & Bibring J P, *Icarus*, 201 (2009) 504.
- 18 Sato T M, Fujiwara H, Takahashi Y O, Kasaba Y, Formisano V, Giuranna M & Grassi D, *Geophys Res Lett*, 38 (2011) 24.
- 19 Montabone L, Forget F, Millour E, Wilson R J, Lewis S R, Cantor B, Kass D, Kleinbohl A, Lemmon M T, Smith M D & Wolff M J, *Icarus*, 251 (2015) 65.
- 20 Aoki S, Giuranna M, Kasaba Y, Nakagawa H, Sindoni G, Geminale A, Formisano V, *Icarus*, 245 (2015) 177.
- 21 Haus R, and Titov D V, *Planet Space Sci*, 48 (12) (2000) 1357.
- 22 Comolli L & Saggin B, *Planet Space Sci*, 58 (2010) 864.
- 23 Smith M D, *Icarus*, 202 (2009) 444.
- 24 Conrath B, Curran R, Hanel R, Kunde V, Maguire W, Pearl J, Pirraglia J, Welker J & Burke T, *J Geophys Res*, 78 (1973) 4267.
- 25 Martin L J, *Icarus*, 57 (1984) 317.
- 26 Martin T Z, *J Geophys Res*, 100 (1995) 7509.
- 27 Haider S A, Batista I S, Abdu M A, Murlikrishna P, Siddi Y S & Kuroda T, *J Geophys Res*, 120 (2015) 8968.